Stout, J. T., & Phillips, R. L. (1973) *Proc. Natl. Acad. Sci. U.S.A. 70*, 3043.
Stout, J. T., & Hurley, C. K. (1977) *Methods Cell Biol. 16*, 87.
Stout, J. T., & Kermicle, J. L. (1979) *Maydica 24*, 59.
Wilson, M. C., & Melli, M. (1977) *J. Mol. Biol. 110*, 511.
Yaguchi, M., Roy, C., Dove, M., & Seligy, V. (1977) *Biochem. Biophys. Res. Commun. 76*, 100.

Investigation of the Structure of Metallothioneins by Proton Nuclear Magnetic Resonance Spectroscopy†

Milan Vašák,* Alphonse Galdes, H. Allen O. Hill,* Jeremias H. R. Kägi, Ian Bremner, and Brian W. Young

ABSTRACT: The proton nuclear magnetic resonance spectra of metallothioneins from horse, human, and sheep livers were investigated. The spectra of the metallothioneins from the three species are similar as are the two isoproteins from any one species. The spectra indicate that metallothioneins possess a well-defined tertiary structure. Zinc(II) and cadmium(II) ions induce similar but not identical tertiary structures. Confirmatory evidence was obtained for the involvement of cysteine residues in metal binding, but no evidence was obtained for the involvement of any other amino acid residue in metal binding. The apoprotein thionein was found to exist essentially in a random-coil conformation with perhaps some residual segmental structure.

Metallothionein is a widely occurring cysteine- and metal-rich protein which was first isolated from the equine renal cortex by Margoshes & Vallee (1957). Other proteins possessing similar properties were subsequently isolated from kidney, liver, and certain other parenchymatous organs of a wide variety of animal species and recently also from a eucaryotic microorganism (Kojima & Kägi, 1978; Lerch, 1979). One of the best characterized metallothioneins is that isolated from equine kidney and liver. The native protein consists of a single polypeptide chain with a molecular weight of 6100 (Kojima et al., 1976). The high metal content [7 g-atoms of Zn(II) and/or Cd(II) per mol of protein] together with the high cysteine content (33%) and the total absence of aromatic amino acids and histidine makes this protein very unusual (Kägi et al., 1974). The biosynthesis of the protein occurs in the liver, kidney, and intestinal wall and is largely accelerated by the administration of metal ions, for example, zinc and cadmium. Consequently, it has been suggested that the protein is involved in metal metabolism, homeostasis, or detoxification (Kojima & Kägi, 1978). Spectroscopic and complexometric titration data have led to the suggestion that the apoprotein (thionein) possesses equivalent and independent binding sites, each containing three cysteinyl residues (Kägi & Vallee, 1961). Furthermore, the sequence shows a distinct clustering of the 20 cysteinyl residues. Within the protein chain the cysteinyl residues occur 7 times in Cys-X-Cys sequences. These sequences have been suggested to be the primary metal binding sites (Kojima et al., 1976). This hypothesis is supported by recent dark field electron microscopy measurements, which have shown that partially denatured metallothionein has a pearl chain structure with six to seven metal ion centers positioned equidistantly along the polypeptide string (Fiskin et al., 1977). The primary structure also reveals that seven of the eight seryl residues occur in -Ser-Cys- sequences.

Table I: Amino Acid Composition of Ovine Metallothioneins 1 and 2

	metallothionein 1[a]	metallothionein 2[a]
cysteine[b]	17.9	19.3
aspartic acid	3.3	3.7
methionine[c]	1.2	1.1
threonine	2.5	2.2
serine	8.8	7.4
glutamic acid	1.3	2.1
glycine	6.9	5.4
alanine	6.1	7.4
isoleucine	0.4	
lysine	7.7	10.0
valine	1.9	2.1
arginine		
proline	*d*	2.1
total	60.1	62.8

[a] Number of residues per M_r 6000. [b] Measured as cysteic acid. [c] Measured as methionine sulfone. [d] Not estimated.

In this paper we report ^{1}H NMR[1] data for metallothioneins isolated from man, horse, and sheep. ^{2}H exchange as well as pH and temperature studies has been used to obtain information about the tertiary structure of the proteins. The results allow tentative conclusions about the function of seryl residues in these proteins. A preliminary account of some of this work has been published (Galdes et al., 1978a,b).

Experimental Section

Materials. Equine liver metallothioneins 1A and 1B (Kojima et al., 1976; Kojima & Kägi, 1978), human liver metallothioneins 1 and 2 (Buhler & Kägi, 1974), and ovine liver metallothioneins 1 and 2 (Bremner & Davies, 1975; Bremner & Marshall, 1974; Bremner et al., 1977) were isolated by a

† From the Biochemistry Department, University of Zurich, 8032 Zurich, Switzerland (M.V. and J.H.R.K.), the Inorganic Chemistry Laboratory, University of Oxford, Oxford OX1 3QR, England, United Kingdom (A.G. and H.A.O.H.), and the Rowett Research Institute, Bucksburn, Aberdeen, AB2 9SB Scotland, United Kingdom (I.B. and B.W.Y.). *Received September 17, 1979.* This work was supported by a Rhodes Fellowship (to A.G.), an E.M.B.O. Fellowship (M.V.), and Swiss National Foundation Grant No. 3.125-0.77. It constitutes part of the program of the Oxford Enzyme Group of which H.A.O.H. is a member.

[1] Abbreviations used: NMR, nuclear magnetic resonance; DSS, 2,2-dimethyl-2-silapentane-5-sulfonate.

0006-2960/80/0419-0416$01.00/0 © 1980 American Chemical Society

combination of gel filtration and ion-exchange chromatography according to established procedures. The primary structures of the equine and human metallothioneins used in the present work have been reported (Kojima et al., 1976; Kissling & Kägi, 1977; Kojima & Kägi, 1978); for the sheep metallothioneins only the amino acid compositions are known and these are given in Table I. Several preparations of each metallothionein, which differed in metal composition, were isolated. ^{2}HCl (99.0% ^{2}H) and NaO^{2}H (99.0% ^{2}H) were from Ryvan Chemical Co., Southampton, U.K., and ^2H_2O (99.7% ^{2}H) was purchased from Merck & Co., Montreal, Canada. All other chemicals were of Analar grade, and buffers were purified from trace metal ions by extraction with dithizone in carbon tetrachloride (Thiers, 1957). Spectropor membrane tubing (Spectrum Medical Industries, Inc., Los Angeles, CA), molecular weight cutoff ~3500, was used for the dialysis of metallothionein samples.

Preparation of Samples. Metallothionein samples were prepared for NMR experiments by dialysis against three changes of 1 mM sodium phosphate buffer, pH 7.5, followed by freeze-drying. The protein was then taken up in 20 mM sodium phosphate buffer, pH 7.5, in either H_2O or ^2H_2O (pH* relates to solutions in ^2H_2O and is the direct meter reading, uncorrected for the ^{2}H isotope effect. All buffered solutions were made by freeze-drying buffers of corresponding pH, prepared in H_2O, and subsequently dissolving the buffer salt in ^2H_2O). The metallothionein samples used in the pH titration studies were dissolved in 20 mM sodium citrate buffer, pH 7.5, rather than sodium phosphate buffer.

The thioneins were prepared by dissolving the freeze-dried metallothioneins in 60 mM HCl followed by dialysis against three changes of the same solution. The resulting thionein was then freeze-dried and taken up in 60 mM HCl–^{2}HCl. The thionein samples used in the pH titration studies were taken up in 60 mM HCl–20 mM citric acid buffer, pH 1.4.

^{1}H NMR Experiments. Pulsed Fourier transform ^{1}H NMR spectra were recorded by using a Bruker 270-MHz spectrometer with an Oxford Instrument Co. superconducting magnet, a Bruker B-NC 12 computer, and a Nicolet 293 pulse controller. The spectrometer was locked on the internal ^2H_2O signal, and for this reason 10% ^2H_2O was added to the samples dissolved in H_2O. Quadrature detection was used, and 1024 free induction decays were routinely accumulated in 4096 data points, over a spectral width of 4 kHz, with a 70° pulse and a 0.6-s separation between consecutive pulses. When accurate relative intensity information was desired, a longer pulse-to-pulse separation (5.0 s) was used in the accumulation of the spectra. The area under the peaks of interest in these spectra was estimated by weighing. For the estimation of the number of protons contributing to the amide proton resonances in H_2O, allowance was made for the 10% ^2H_2O present, on the assumption that no equilibrium isotope effect is present (Hvidt & Nielsen, 1966). The temperature of the probe cavity was controlled to within ±1 °C with a Bruker temperature control accessory. The probe temperature was calibrated by using a copper–constantan thermocouple (Comark Electronic Ltd.). Unless otherwise indicated, spectra were collected at 28 °C. Difference spectra and convolution difference spectra (Campbell et al., 1973, 1974) were used to aid resolution. Spin–echo spectra were obtained as described in the literature (Campbell et al., 1975a). Chemical shifts are reported relative to sodium 2,2-dimethyl-2-silapentane-5-sulfonate (DSS) as an internal standard. Typically, samples for NMR experiments contained 1–5 mM protein in 0.4 mL of the indicated buffer system.

The solvent water signal was suppressed by applying a gated pulse at the appropriate frequency at all times except during data acquisition (Campbell et al., 1975b, 1977). The suppresion of the very intense water signal is essential when H_2O is used as a solvent (Campbell et al., 1975b), but it will result in a loss of intensity for resonances associated with exchangeable protons (Campbell et al., 1977); this is referred to as saturation transfer. In peptides and proteins saturation transfer to the amide protons is frequently observed under these conditions (Glickson et al., 1974; Campbell et al., 1975b; Bundi & Wüthrich, 1977). For saturation transfer to be observed, the exchange rate (k) of the labile protons must be larger than T_1^{-1}, where T_1 is the spin–lattice relaxation time of the protons concerned (Brown & Campbell, 1976; Campbell et al., 1977). For amide protons this condition means that saturation transfer will be observed when $k \gtrsim 1\ s^{-1}$. The extent of saturation transfer under these conditions is also dependent on k, according to the equation $I_s = I_0/(1 + T_1k)$, where I_0 is the resonance intensity in the absence of saturation transfer and I_s is the minimum resonance intensity in the presence of saturation transfer.

The exchange rates of the slowly exchanging labile protons in ^2H_2O were determined by recording the spectra at different times after dissolving the protein in ^2H_2O and measuring the intensity of the peaks of interest. The pseudo-first-order rate constants for the exchange reactions were calculated from these data by using the usual semilogarithmic plots of intensity against time.

In pH titration experiments, the pH was altered by the addition of small volumes (~5 μL) of 0.5 M HCl–^{2}HCl or 0.5 M NaOH–NaO^{2}H, such that the ^{2}H content of the sample was kept constant. The pH* (or pH) was measured with a Pye Ingold microelectrode fitted to a Radiometer 26 pH meter. The maximum chemical shift difference between the protonated and unprotonated species and the pK_a value for the titrating residue were obtained from a direct linear plot as described by Browne et al. (1976).

Results and Discussion

General Features of the Spectra. Representative ^{1}H NMR spectra in the 0–5-ppm region (i.e., upfield of the solvent signal) for the metallothioneins and corresponding thioneins studied in this work are given in Figures 1 and 2, respectively. The spectra obtained for the metallothioneins (and thioneins) from the three species investigated are exceedingly similar. This is consistent with the extensive sequence homology reported for some of these proteins (Kojima & Kägi, 1978). In the low-field region, 6–10 ppm, a series of broader resonances are observable when the spectra are recorded in H_2O (Figures 3 and 9). These low-field resonances are absent when the spectra are recorded in ^2H_2O.

Assignment of Resonances. As a starting point for the assignment of the observed ^{1}H NMR resonances, the spectra can be divided into three distinct regions, each region being characteristic of a particular type of hydrogen atom (Campbell et al., 1975c). Thus, in the absence of aromatic amino acids and histidinyl residues, the resonances to low field of the solvent, between 7 and 10 ppm, mainly arise from amide protons (Wyssbrod & Gibbons, 1973; Campbell et al., 1975c). This assignment is confirmed by the exchange of the protons responsible for these resonances with solvent deuterons when the metallothioneins and thioneins are dissolved in ^2H_2O. The next distinct region is that due to the α-C proton resonances, which occur in the 3.5–5.5-ppm region, and the resonances in the 0.7–3.8-ppm region can be assigned to the side-chain protons (Wyssbrod & Gibbons, 1973; Campbell et al., 1975c).

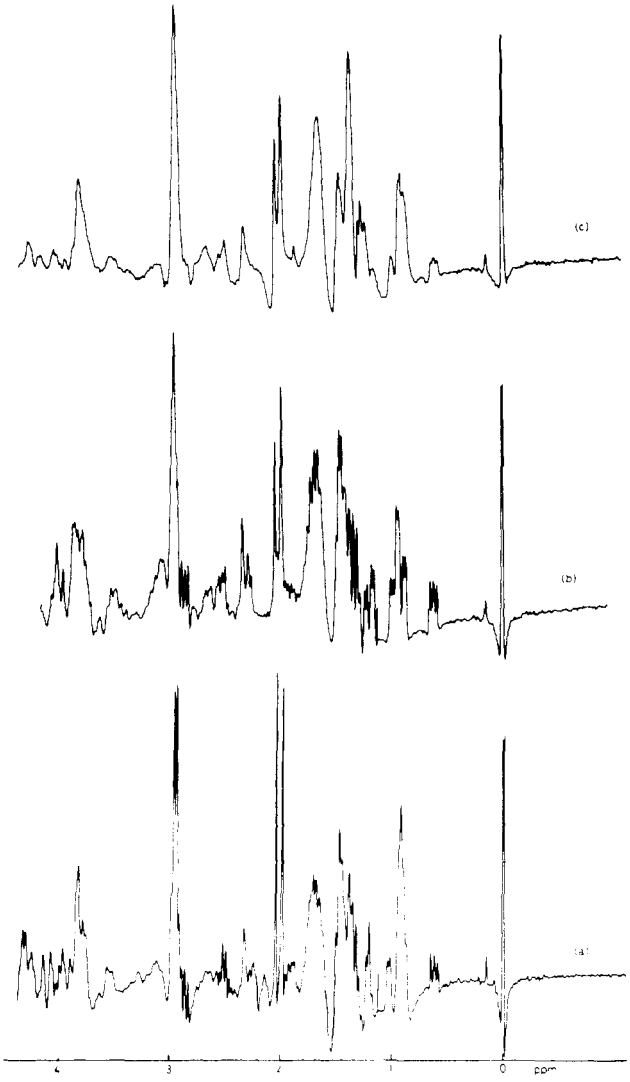

FIGURE 1: 270-MHz ^1H NMR convolution difference spectra in the high-field region of metallothioneins. (a) Equine metallothionein 1B (metal composition 25% cadmium and 75% zinc); (b) ovine metallothionein 2 (metal composition 100% zinc); (c) human metallothionein 2 (metal composition 100% zinc). All three samples were dissolved in sodium phosphate buffer (20 mM) in ^2H_2O, pH* 7.5, and had a final concentration of 1 mM. The resonance at 0 ppm is due to the internal standard (DSS).

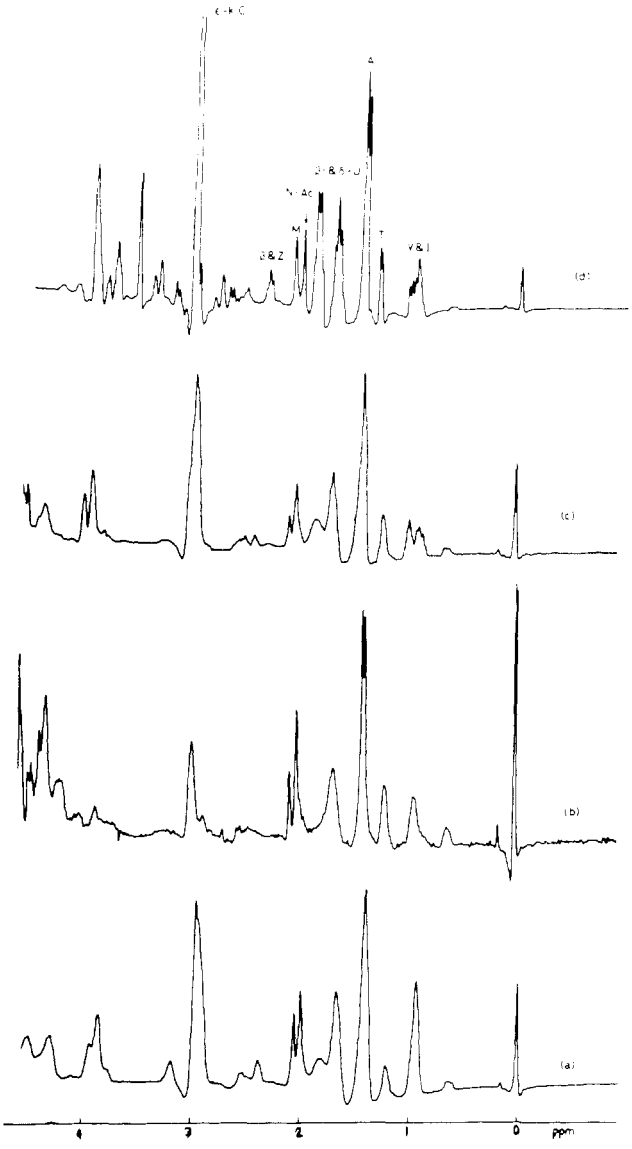

FIGURE 2: 270-MHz ^1H NMR convolution difference spectra in the high-field region of thioneins. (a) Equine thionein 1B; (b) ovine thionein 2; (c) human thionein 2; (d) an amino acid mixture having the same composition as human thionein 2. The resonance marked DSS is from the internal standard, and the other labels refer to the main amino acid residues contributing to the marked resonances. All samples were in ^2HCl (60 mM). Samples a, b, and c were dissolved in 60 mM ^2HCl and had a final concentration of 1 mM.

In a random-coil protein, the resonances in the side-chain region can be assigned to specific protons by a comparison of the observed spectra with the assigned spectra of the constituent amino acids (McDonald & Philips, 1969; Roberts & Jardetzky, 1970; Campbell et al., 1975c). In a folded protein these resonances can be shifted by up to a few parts per million from their primary position. However, these secondary shifts arise mainly from ring currents of aromatic amino acids (Dwek, 1973; Campbell et al., 1975c), and hence, in the absence of such residues, shifts of a much smaller magnitude are to be expected. Therefore, the side-chain resonances are assigned as a first approximation to amino acid type by a comparison of the observed spectra with the spectra of the constitutent amino acids. Indeed, the observed spectra for the thioneins are practically indistinguishable from the spectra obtained for mixtures of the constitutent amino acids of the same composition (Figure 2). This similarity extends not only to the chemical shift position of the resonances but also, more importantly, to their relative intensities. In fact, the estimated number of protons under each of the main peaks in the thionein spectra is in accord with that expected from such an assignment procedure. The spectra obtained for the metallothioneins (Figure 1), though similar to the spectra obtained for the corresponding amino acid mixtures and the thioneins (Figure 2), show that some of the resonances occur over a wider range of chemical shift values. However, even in the *metallo*thioneins the observed resonances are not markedly perturbed from their primary chemical shift positions and can be assigned accordingly. This assignment to amino acid type can be made with particular confidence for resonances which are isolated from nearby resonances, such as the valine CH_3 (0.9 ppm) and the cysteine β-CH_2 (3.0 ppm) resonances (Figures 1 and 2).

The spectral properties of the metallothioneins and thioneins will now be considered in some detail, with particular attention given to the amide region of the spectra. Most of the experiments described in subsequent sections were performed on the two equine metallothioneins and on at least one of the two ovine metallothioneins. Since the results were in each case the same, this work will be mainly illustrated by reference to equine metallothionein 1B, which is the best characterized of

Table II: Some Properties of the Amide Protons in Equine Metallothionein 1B[a]

peak	δ (ppm)[b]	no. of protons estimated (% of total obsd)[c]	dδ/dT[d] (ppb/°C)	intensity loss/dT (%/10 °C)	$t_{1/2}$ for H exchange (min)[c]
A	9.60	2.0	3.6 ± 0.4	15–20	<2.4
B	9.47	1.6	3.9 ± 0.3	15	<2.4
C	9.24	1.6	2.2 ± 0.5	20–25	<2.4
D	9.00	7.6	1.1 ± 0.2	5	300
E	8.81	5.1	0.3 ± 0.1	5	30
F_1	8.73	5.1[e]	0.3 ± 0.2	10	17
F_2	8.73		2.3 ± 0.4	20	
G_1	8.55	13.5[e]	0.3 ± 0.3	5	23
G_2	8.52		2.2 ± 0.3	15–20	
H	8.31	11.4	2.9 ± 0.2	10	23
J	7.47	3.3	0.1 ± 0.1	35	<2.4
K	7.40	10.0	1.9 ± 0.1	5–10	60
L	7.07	6.2	0.7 ± 0.1	5	315
M	6.81	2.4[e]	3.4 ± 1.6	40–45	<2.4
N	6.77		1.5 ± 0.4	40–45	<2.4
f	8.20–7.60	~30			

[a] The metal composition of the sample was 15% cadmium and 85% zinc. The sample was dissolved in 20 mM sodium phosphate buffer, pH* 7.5, in 90% H_2O–10% ^2H_2O, except for the H/^{2}H exchange experiment, for which the sample was in ~100% ^2H_2O. The amide peaks are labeled as in Figures 3 and 4. [b] At 28 °C. [c] At 15 °C; calculated from the total area of low-field resonances corresponding to 26 out of a theoretical total of 65 amide protons (see text). [d] Plus or minus standard error; calculated by least-squares analysis from the data in Figure 4. [e] Resonances overlapping. [f] Unresolved region.

the metallothioneins studied (Kojima et al., 1976).

Metallothionein Spectra. Structure of Metallothionein. When the spectra of a solution of metallothionein, dissolved in H_2O, are collected, a broad band of amide protons extending from 9.6 to 6.8 ppm can be observed (Figures 3 and 6). When the holoprotein is dissolved in ^2H_2O, the bulk of these amide protons rapidly exchanges with the solvent ($t_{1/2} < 2.4$ min; Figure 3 and Table II), but up to 12 residual amide peaks, with significantly slower exchange rates ($t_{1/2} \simeq 20$–320 min; Figure 3 and Table II), can be observed. The difference in the exchange rates for the amide protons in metallothionein is also evident from the extent of saturation transfer of the different amide protons in H_2O. Thus, at 15 °C the total number of protons in the low-field region for equine metallothionein 1B, dissolved in 20 mM sodium phosphate buffer–H_2O, pH 7.5, is estimated to be 26 vs. 65 expected from the primary structure of this metallothionein (Kojima et al., 1976). We attribute this to saturation transfer from the H_2O solvent to a considerable number of the amide protons under these conditions. This is consistent with the expected exchange rate of solvent-exposed amide protons at this pH ($k \simeq 15$ s^{-1}; Hvidt & Nielsen, 1966; Molday et al., 1972). The remaining amide proton resonances in this spectrum have been divided into 13 distinct peaks (Figure 3). Since many of the peaks are probably associated with more than one proton, the properties of these resonances (vide infra) will represent the average properties of the contributing protons. When the temperature is raised from 15 to 75 °C, the amide proton resonances show a large decrease in intensity and an upfield shift (Figures 3 and 4); in general, those peaks which show the larger shifts lose intensity much more rapidly than peaks which show small shifts (Figure 4 and Table II). The observed temperature-dependent chamical shifts (0.1–4 ppb/°C; Table II) are all lower than that expected for a solvent-exposed amide proton (6–7 ppb/°C; Kopple et al., 1972), suggesting that the observed protons are to some extent solvent inaccessible. In

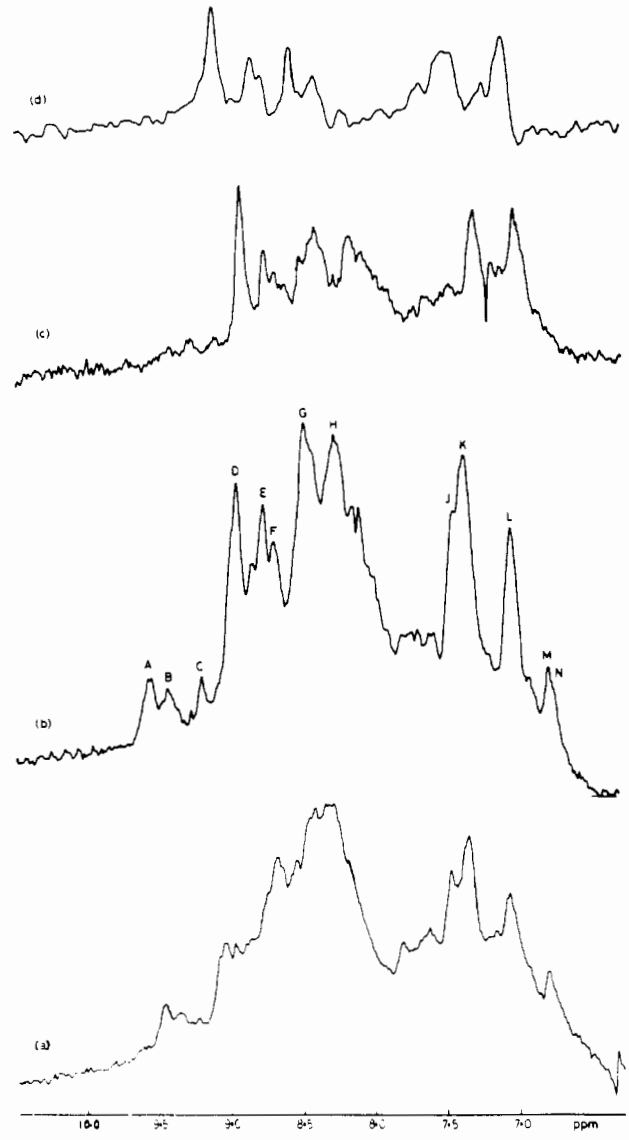

FIGURE 3: 270-MHz ^{1}H NMR spectra in the low-field region of equine metallothionein 1B (2 mM) in sodium phosphate (20 mM) buffer, pH 7.5. (a) Metal composition 59% cadmium and 41% zinc; in H_2O at 28 °C; (b) metal composition 25% cadmium and 75% zinc; in H_2O at 28 °C. The labeling refers to distinct amide peaks, as described in the text. (c) As (b) but at 64 °C; (d) as (b) a few minutes after dissolving in ^2H_2O at 15 °C.

particular, the peaks which show little intensity loss and small temperature-dependent chemical shifts (Figure 4 and Table II) must be very inaccessible to the solvent. Indeed, the chemical shifts of these amide protons are similar to those of the slowly exchanging protons in ^2H_2O (Table II). The observation of these solvent-inaccessible amide protons indicates the presence of an inner core of amide protons shielded from the solvent in a folded protein structure (Wagner et al., 1978). Hence, it is concluded that, contrary to previous reports (Rupp et al., 1974), metallothionein possesses a well-defined tertiary structure. This is also demonstrated by the large chemical shift span, ~3 ppm, over which the amide protons resonate in metallothionein (Figure 2), a situation which can only arise if different amide protons experience different chemical/magnetic environments depending on their position in the folded protein. As mentioned above, the side-chain proton resonances in metallothionein show small, but significant, differences in chemical shift position from the corresponding resonances in the thionein or the constituent amino acid spectra (Figures 1 and 2). This is consistent with a folded structure

Table III: ^{1}H NMR Chemical Shifts for the Slowly Exchanging Amide Protons in ^2H_2O for Equine Metallothioneins[a]

	metal contents		chemical shift (ppm)										
	% Cd	% Zn											
equine metallothionein 1A	2	98[b]	9.04				8.31						
	25	75[c]	9.09		8.76	8.58		7.68	7.54	7.43	7.24	7.10	7.05
	55	45	9.09					7.69	7.56	7.39			
	62	38	9.07					7.69	7.54	7.37	7.32		
equine metallothionein 1B	15	85[c]	9.09	8.83	8.77	8.57	8.39	7.68	7.53	7.44	7.22	7.14	7.09
	59	41	9.09					7.65	7.53			7.08	7.05
	59	41[d]	9.09					7.65			7.20		7.05

[a] The metallothionein was in 20 mM sodium phosphate–^2H_2O buffer, pH* 7.5, at 28 °C, unless otherwise indicated. Unless indicated otherwise, the spectra were obtained after a few minutes of making up the sample in ^2H_2O, except for footnote *b*. [b] After 2 h of dissolving in ^2H_2O. [c] At 15 °C. [d] Reconstituted metallothionein following metal removal by exposure to low pH (see text for details).

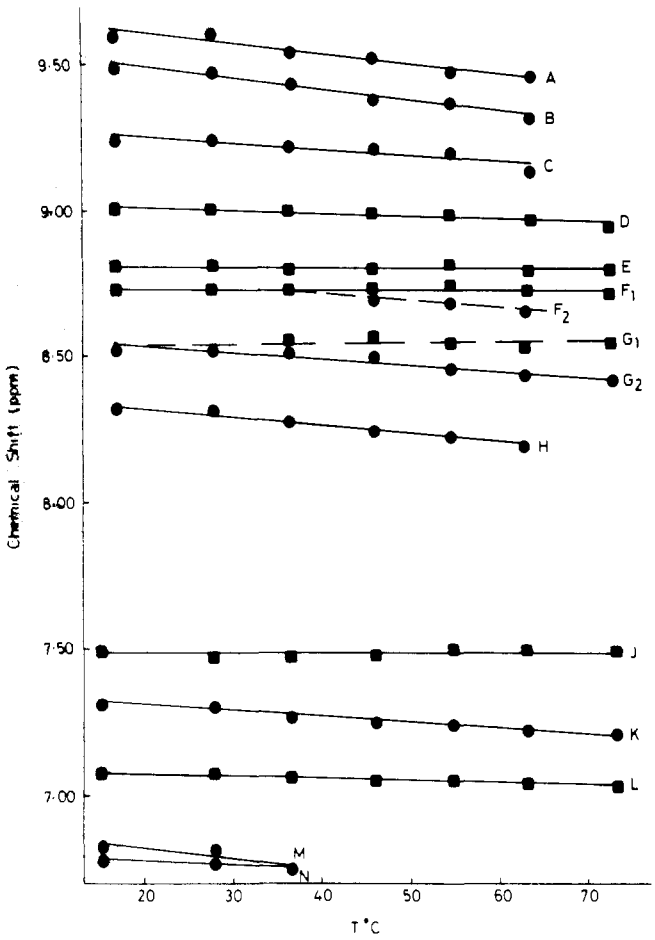

FIGURE 4: Plot of chemical shift vs. temperature for the amide peaks of equine metallothionein 1B. The sample was in 20 mM sodium phosphate–H_2O buffer, pH 7.5. The labeling is as in Figure 3b.

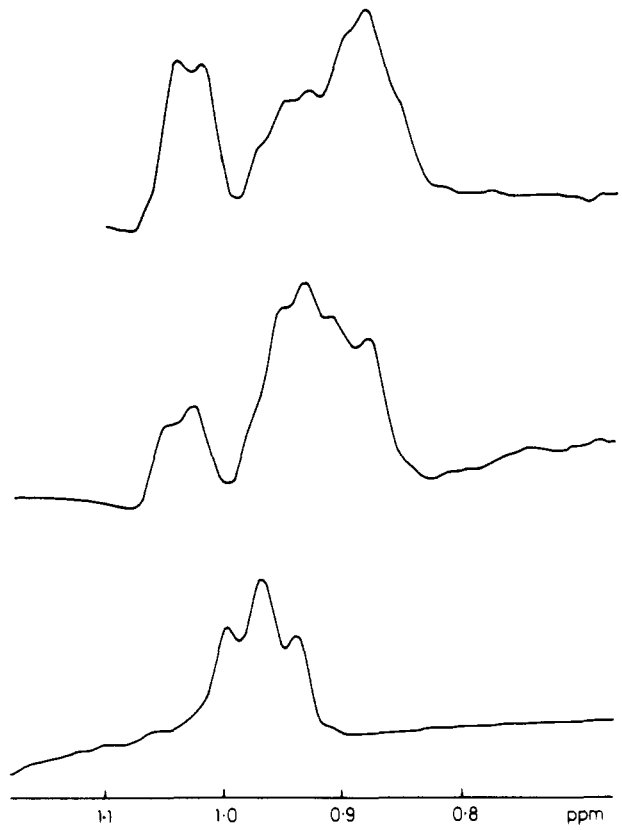

FIGURE 5: 270-MHz ^{1}H NMR convolution difference spectra in the upfield region for equine metallothionein 1A (2 mM) in sodium phosphate (20 mM) buffer in ^2H_2O at pH 7.5. The metal composition was (bottom) 2% cadmium, 2% copper, and 96% zinc, (middle) 25% cadmium and 75% zinc, and (top) 55% cadmium and 45% zinc.

for metallothionein (Campbell et al., 1975c). Some of the side-chain resonances appear to be affected to a greater extent than others. Thus, though the methionyl (2.08 ppm), *N*-acetyl (2.02 ppm), and threonyl (1.22 ppm) methyl resonances are unperturbed, the alanyl methyl resonances are markedly affected (Figures 1 and 2). In the thionein (or constituent amino acid) spectra the resonances from all the methyl groups of the alanine residues (5–7 in those species investigated) are superimposed and occur at 1.41 ppm; in the metallothionein spectra these resonances are no longer superimposed but occur between 1.5 and 1.3 ppm.

Consequences of Metal Binding to Metallothionein. The overall pattern of the amide proton resonances in metallothioneins in H_2O depends on the metal ion composition of the sample (parts a and b of Figure 3). The chemical shifts of some of the slowly exchanging amide protons in ^2H_2O for equine metallothioneins are listed in Table III. The existence of some definite variation in the position of the resonances and in their intensities (not shown) suggests that Cd(II) and Zn(II) ions induce a similar, but not identical, tertiary structure perhaps as a consequence of the different sizes and/or coordination preferences of these metal ions. The effects of metal composition on the spectrum also indicate that the Cd(II)- and Zn(II)-containing proteins do not constitute a mixture of Zn(II) metallothionein and Cd(II) metallothionein but that the two metal ions are part of the same molecule. If this were not the case, no variation in chemical shift would be expected for the amide protons at different metal ion compositions. Some of the side-chain resonances also seem to reflect the metal ion composition of the protein. This is particularly striking for the resonance assigned to the methyl group of the sole valyl residue in equine metallothionein 1A. In the zinc-only protein one peak, at 0.97 ppm, is observed for this reso-

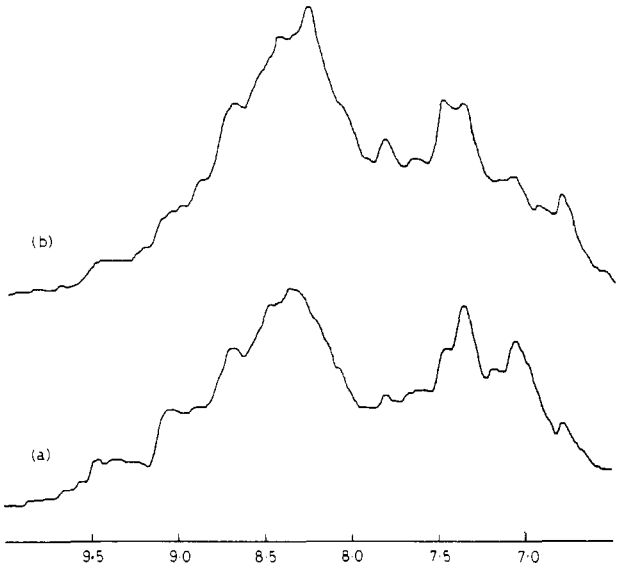

FIGURE 6: 270-MHz ^1H NMR spectra in the low-field region for equine metallothionein 1B (3 mM) (metal composition 59% cadmium and 41% zinc) in sodium citrate (20 mM) buffer–H_2O (a) at pH 7.5 before pH titration and (b) at pH 7.0 after titration down to pH 1.4.

nance (Figure 5), whereas in the presence of cadmium two additional peaks, at 1.03 and 0.88 ppm, are observed (Figure 5). The relative intensity of these peaks parallels the cadmium content of the protein (Figure 5), with the 1.03- and 0.88-ppm peaks becoming progressively more intense as the cadmium content increases. This valyl residue is located at position 49 of the primary structure, between two cysteinyl residues (Kojima & Kägi, 1978). As mentioned above, such Cys-X-Cys sequences have been suggested to be the primary metal chelation sites in metallothioneins (Kojima et al., 1976), and the observed large perturbation of Val-49 on metal substitution is entirely consistent with such a view. This valine residue is conserved in equine metallothionein 1B (Kojima et al., 1976), and indeed peaks at 1.03 and 0.88 ppm, whose intensity is dependent on the Cd(II)/Zn(II) ratio, are also evident in the spectra of this metallothionein. However, since two additional valyl residues (not associated with any of the Cys-X-Cys sequences) are also present in equine metallothionein 1B, the assignment of the metal-sensitive peak to Val-49 cannot be made with complete confidence.

pH Titration of Metallothionein. When the pH of a solution of equine metallothionein 1B, containing both zinc and cadmium, in 20 mM citrate–H_2O buffer is lowered from about pH 7.0 to 1.4, the metals are released (Kägi & Vallee, 1960, 1961). This process is accompanied by a gradual decrease in the intensity of the amide resonances typical of the holoprotein and a concomitant increase in the resonance positions typical of the apoprotein. The high-field resonances also change from the metallothionein position to the thionein position. When the pH is raised back to pH 7.0, the spectrum of the holoprotein is regenerated. The upfield region of the regenerated spectrum appears identical with that of the original spectrum whereas the amide region of the regenerated holoprotein, though very similar, is not identical with that in the original spectrum (Figure 6). When the regenerated sample, after freeze-drying, is then taken up in ^2H_2O, the positions of the resonances of some of the slowly exchanging amide protons are different from those of the original sample (Table III). The close similarity of the original and the regenerated metallothionein spectra demonstrates that the native tertiary structure of metallthionein is largely restored when the metals are reintroduced into the thionein, the small differences in the

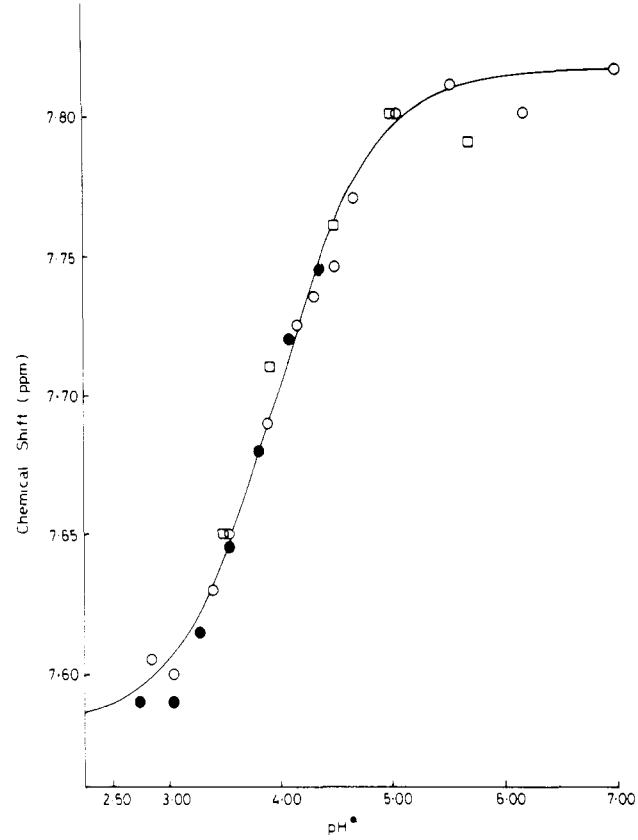

FIGURE 7: Titration curve for pH-dependent amide resonance in equine 1B. The samples were dissolved in sodium citrate buffer (20 mM) and had a final concentration of 3 mM. The experimental values of chemical shift are shown by symbols, and the line is a theoretical curve for a pK_a of 4.0 and a span of 0.24 ppm. Symbols: (●) metallothionein, pH titrated from high pH to low pH; (○) metallothionein, pH titrated from low pH to high pH; (□) thionein, pH titrated from low pH to high pH.

amide region of the spectra of the original and regenerated samples being of the order expected if some scrambling of the Cd(II) and Zn(II) occurred.

A resonance arising from an amide proton titrates reversibly with change in pH (Figure 7) with an associated pK_a of 4.0. The same phenomenon is also observed in the pH titration of ovine metallothionein 1. The large change in chemical shifts observed (0.24 ppm; Figure 7) suggests that this behavior is associated with the protonation of the carboxylic group of the C-terminal residue (alanine in equine metallothionein; Kojima & Kägi, 1978). The titration of the glutamyl δ-carboxylic and aspartyl γ-carboxylic groups is expected to result in changes in chemical shifts of less than 0.05 ppm for the corresponding amide proton (Bundi & Wüthrich, 1977). Since this titrating proton is also present in ovine metallothionein, with an identical pK_a and chemical shift position as that in the equine metallothionein, it seems likely that the C termini of both species are identical.

Nature of the Metal-Binding Ligands. A comparison of the spin–echo spectra for metallothionein and thionein reveals a large difference in the behavior of the cysteinyl β–CH_2 resonances (Figure 8). The phase of these resonances in thioneins and metallothioneins is very different, whereas the phase of all the other resonances is similar. The phase of the spin–echo spectrum is sensitive to the spin–spin coupling of the nuclei responsible for the observed resonance (Campbell et al., 1975a; Campbell & Dobson, 1975). Therefore, the observed phase difference between the thionein and the metallothionein spin–echo spectra must have its origin in grossly

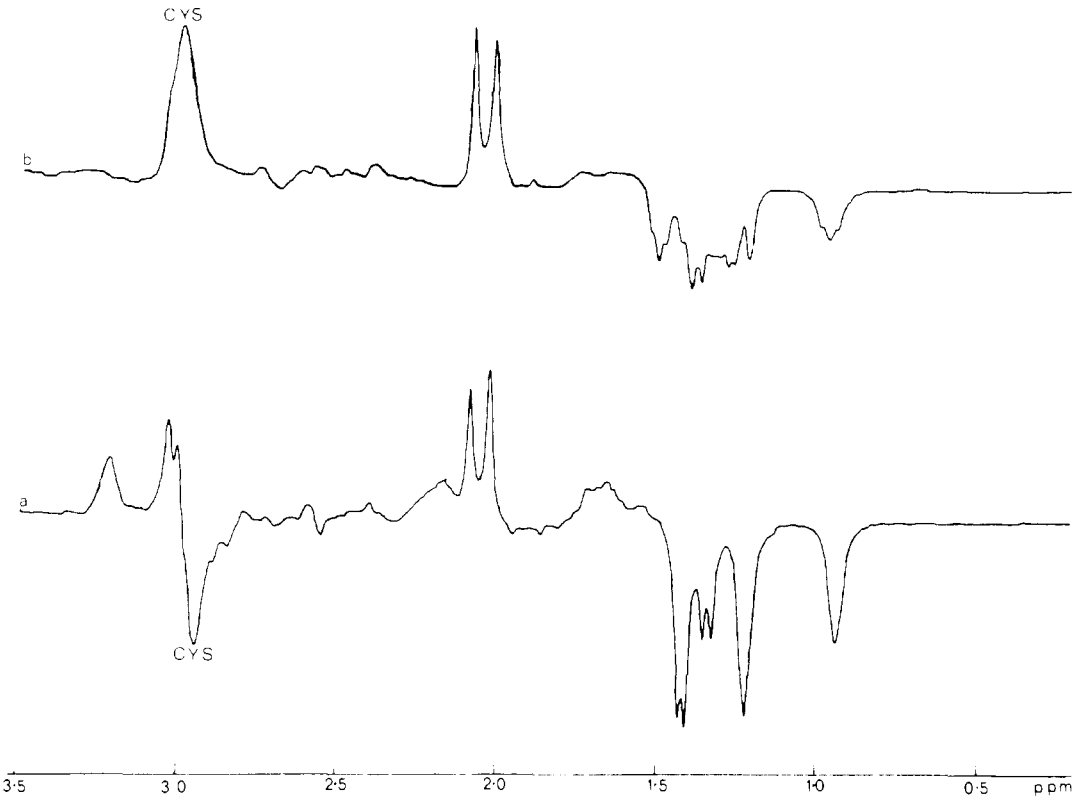

FIGURE 8: 270-MHz ^1H NMR spin-echo spectra of equine metallothionein 1A. (a) Equine thionein (2 mM) in sodium phosphate (100 mM) buffer in ^2H_2O, pH* 7.5; (b) equine metallothionein (2.5 mM) (96% zinc) in sodium phosphate (20 mM) buffer in ^2H_2O, pH* 7.3. The pulse sequence employed is $90°-\tau-180°-\tau$-collect with τ = 71 ms.

different spin–spin coupling of the cysteinyl β-CH_2 protons to the corresponding α-C proton and to each other in the two proteins. This is consistent with the proposed role of the cysteinyl residues as the metal binding sites in metallothioneins (Kägi & Vallee, 1960, 1961). As to the nature of any other ligands (aside from the cysteines), no evidence was obtained in the present study implicating any other residue as a metal ligand. The total invariance in chemical shift of the methionyl S–CH_3 protons in the apoprotein and in the holoprotein (Figures 1, 2, and 8) is inconsistent with the proposed role (Sadler et al., 1978) of the methionyl sulfur groups as one of the metal-binding ligands.

Thionein Spectra. In the low-field region of the spectra of thionein in 60 mM HCl, the amide protons occur in two main peaks (Figure 9). The position and intensity of these peaks are temperature dependent (see below). At 28 °C the first peak (I) which is quite broad, is centered around 8.3 ppm (width at base ~0.4 ppm) while the second peak (II), which is much sharper, is found at 7.51 ppm (Figure 9b). An additional small peak (III) is seen at 7.18 ppm in equine metallothioneins only.

When the thionein is dissolved in ^2HCl, all of these amide protons exchange rapidly with the solvent, with the protons contributing to peak II exchanging at least an order of magnitude faster than those contributing to peak I (Table IV). Thus, 3 min after dissolving the thionein in 30 mM ^2HCl at 5 °C, over 80% of peak I is still present while the protons contributing to peak II have nearly exchanged completely (Figure 9). The measured exchange rate for the thionein amide protons in ^2HCl (Table IV) suggests that saturation transfer from the solvent to the protons contributing to peak II, but not to peak I, may occur when the spectra are measured in HCl (see Experimental Section). (Only a lower limit for the exchange rate of the protons contributing to peak II could be obtained.)

Table IV: Some Properties of the Amide Protons in Equine Thionein 1B[a]

peak	chemical shift (ppm)[b]	no. of protons[c]	$d\delta/dT$ (ppb/°C)[d]	$t_{1/2}$ for H/^{2}H exchange (min)[e]
I	8.1–8.5	45	6.1 ± 0.2	17
II	7.51	17	3.3 ± 0.2	<1
III	7.18	1	2.5 ± 0.1	

[a] In 60 mM HCl, except for footnote *e*. [b] At 28 °C. [c] At 5 °C; peak III was taken as equivalent to 1 proton. [d] Plus or minus standard error; calculated by least-squares analysis from the data in Figure 10. [e] Determined at 5 °C in 30 mM ^2HCl solvent.

When the temperature of a solution of thionein in 60 mM HCl is raised from 5 to 80 °C, an upfield shift, accompanied with a loss of intensity, is seen for all the low-field protons (Figures 10 and 11). The loss of intensity can be attributed to an increase in the exchange rate which again results in an increase of saturation transfer with the solvent. The shift is greater for peak I, while the loss of intensity is more pronounced for peak II (Figures 9–11 and Table IV). The latter observation is consistent with the higher exchange rate of peak II (Table IV). In the aliphatic region some of the peaks sharpen, but no change in the chemical shifts is observed with increasing temperature. The temperature-induced changes are fully reversible over the temperature range studied.

When the pH of a solution of thionein in 20 mM sodium citrate buffer–H_2O is raised from pH 1.4 to 7.0, no change in peak position is observed for either of the two amide peaks. However there is a dramatic loss of intensity for both peaks (Figures 9 and 12), consistent with the known rapid increase in the exchange rate of peptide amide protons and labile amino acid side-chain protons above pH 3.0 (Hvidt & Nielsen, 1966; Molday et al., 1972; Bundi & Wüthrich, 1979a,b). The loss

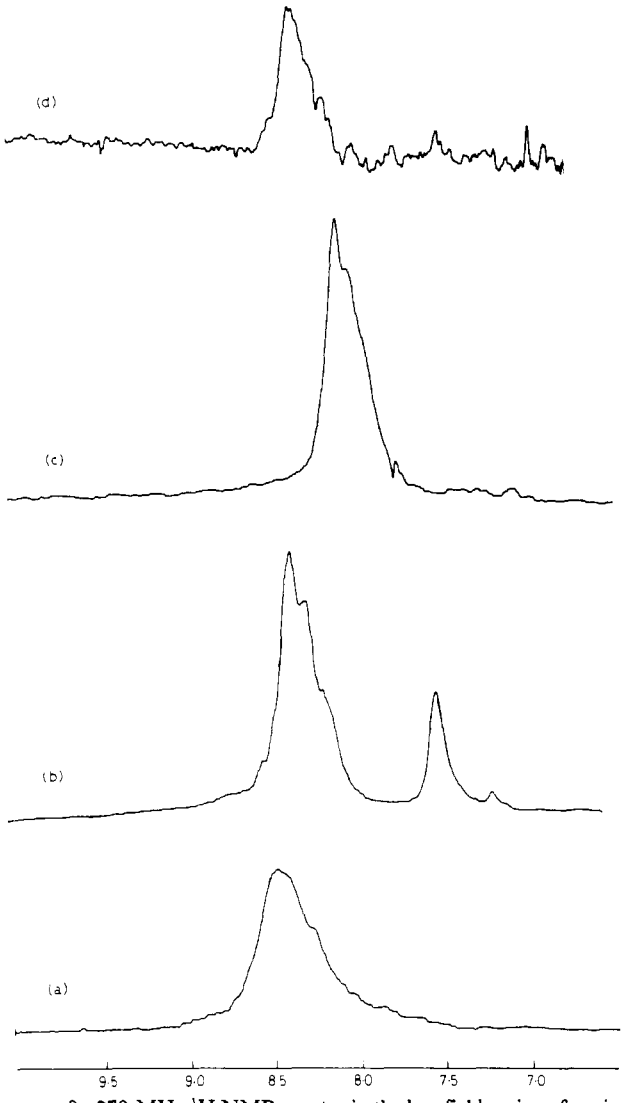

FIGURE 9: 270-MHz ^1H NMR spectra in the low-field region of equine thionein 1B (3 mM). (a) 3 min after dissolving in 30 mM ^2HCl, 5 °C; (b) in 60 mM HCl, 28 °C; (c) in 60 mM HCl, 73 °C; (d) in 20 mM sodium citrate–H_2O buffer, pH 4.5, 28 °C.

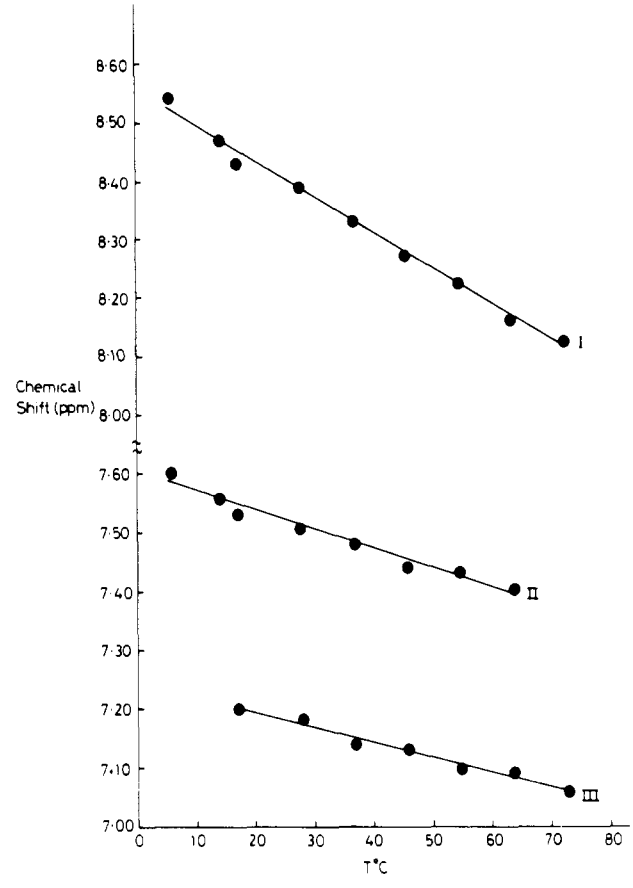

FIGURE 10: Plot of chemical shift vs. temperature for the amide protons of equine thionein in 60 mM HCl. The labeling is as in Table IV.

of intensity is again more pronounced for peak II, so that by pH 4.5 this peak is virtually absent while peak I is still clearly visible (Figure 9d). As the pH is raised, one amide peak is seen to shift downfield from underneath peak II, at 7.51 ppm, to 7.80 ppm with a pK_a of ~4.0 (Figure 7). In the upfield region there is no change in peak position with pH for any of the observed resonances, with the sole exception of a single resonance which titrates upfield from underneath the alanyl CH_3 peak at 1.41 to 1.33 ppm, again with a pK_a of ~4.0. The titrating amide peak is identical in chemical shift position and pK_a with those observed in the holoprotein (Figure 7) and can, on the same arguments (see above), be assigned to the C-terminal alanine residue. This assignment is confirmed in the thionein by the direct observation of a titrating alanyl β-CH_3 resonance over the same pH range and with an identical pK_a.

Thionein Structure. The above results suggest that thionein, in marked contrast to metallothionein has a much less well-defined tertiary structure. The similarity of the upfield region of the thionein spectra with the spectrum of a mixture of the constituent amino acids (Figure 2) and the observation of most of the low-field protons of the thionein in one major band between 8.5 and 8.1 ppm (Figure 9 and Table IV) are clear indications that thionein is in a random-coil conformation in the sense that most of the amino acid side chains are exposed to the solvent. In addition, the measured temperature-dependent chemical shift for the major peak (6 ppb/°C; see Table IV) is that expected for solvent-exposed amide protons (Kopple et al., 1972), and the measured $H/^2H$ exchange rate at 5 °C for the protons contributing to this peak (~0.05 min^{-1}; see Table IV) in equine thionein 1B is not too different from that estimated for the random-coil protein (~0.1 min^{-1}). The latter value was calculated from the amino acid sequence of this thionein (Kojima et al., 1976) by using the empirical procedure of Molday et al. (1972) and utilizing the value of the $H/^2H$ exchange rate for poly(DL-alanine) given by Hvidt & Nielsen (1966). The other two peaks (peaks II and III in Figures 9 and 12, Table IV) in the low-field region of thionein can be assigned for the most part to labile side-chain proton resonances. Peak III at 7.18 ppm is only seen in the equine forms of metallothionein and can be attributed to the labile protons of arginyl residues found only in the horse protein but not in the human and ovine forms. The chemical shift coincides with that for arginine-containing model peptides (Bundi & Wüthrich, 1979a,b). Most of the intensity of peak II at 7.51 ppm arises from the ϵ-amino group of the seven lysyl residues (Bundi & Wüthrich, 1979a,b) and from the three primary amide groups (Glickson et al., 1974; Bundi & Wüthrich, 1979a,b; Brewster & Hruby, 1973) present in equine metallothionein 1B (Kojima et al., 1976). In addition, as judged from the above-mentioned effect of the titration of the C-terminal carboxylic acid group on a proton resonance in this spectral region (Figure 7), at least one backbone peptide hydrogen is also hidden underneath peak II. The displacement of peptide hydrogens to higher field would be indicative of residual hydrogen bonding since similar shifts of peptide hydrogen resonances have been reported for oligopeptides forming β-turn and pleated sheet structures (Kopple et al., 1969; Urry

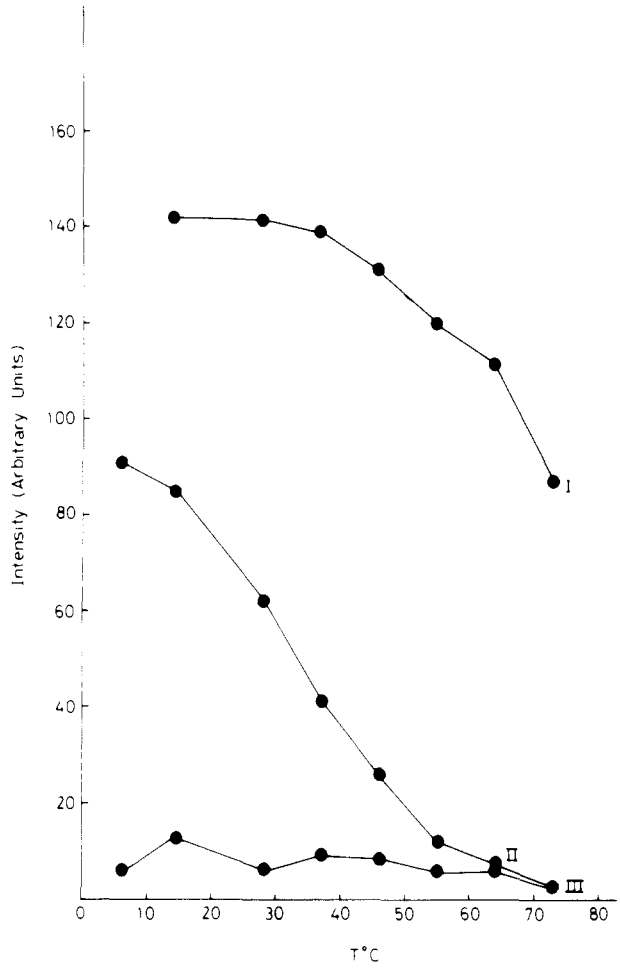

FIGURE 11: Plot of intensity vs. temperature for the amide protons of equine thionein 1B in 60 mM HCl. The labeling is as in Table IV.

et al., 1970; Von Dreele et al., 1971, 1978). Downfield shifts of the resonances upon deprotonation of a nearby carboxyl group (Figure 7) have been observed also in a number of hydrogen-bonded model peptides (Bundi & Wüthrich, 1979a,b).

A chemical shift of 7.51 ppm is, however, rather low for the common type of hydrogen bonding to main-chain carbonyl acceptors. Plausible alternative candidates for forming stable hydrogen bonds to the backbone secondary amide groups are, however, the oxygen atoms of amino acid side chains. Indeed, as shown previously for myoglobin (Richards, 1963), the numerous serine side-chain oxygens in the primary structure of metallothionein could serve as readily available acceptors for such side-chain–main-chain hydrogen bonds. Thus, a hydrogen bond to the next nearest seryl residue could explain the position and the titration behavior of the pH-sensitive C-terminal peptide proton.

Conclusions

The main conclusions of the present work can be summarized as follows. (1) Great similarity exists between metallothioneins from different species and between the two isoproteins from within a particular species. (2) Metallothionein possesses a well-defined tertiary structure. (3) Different metal ions induce similar but not identical tertiary structures. (4) No evidence was obtained for any amino acid residue other than the cysteinyl thiol groups acting as metal-binding ligands. (5) The thioneins exist in a random-coil conformation which nevertheless may possess some segmental structure.

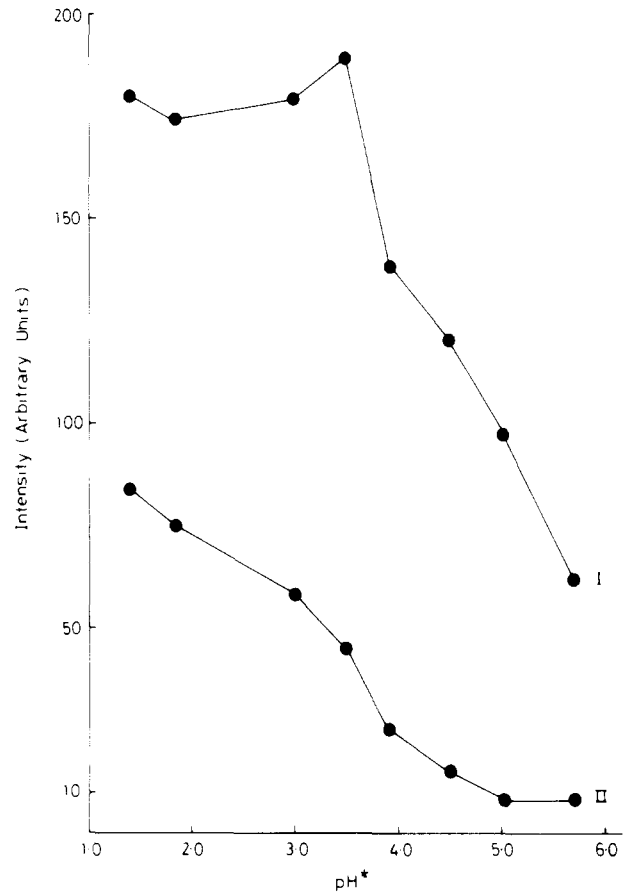

FIGURE 12: Plot of intensity vs. pH for the amide protons of equine thionein 1B (3 mM) in sodium citrate (20 mM) buffer in H_2O. The labeling is as in Table IV.

References

Bremner, I., & Marshall, R. B. (1974) *Br. J. Nutr. 32*, 293.
Bremner, I., & Davies, N. T. (1975) *Biochem. J. 149*, 733.
Bremner, I., Williams, R. B., & Young, B. W. (1977) *Br. J. Nutr. 38*, 87.
Brewster, A. I. R., & Hruby, V. J. (1973) *Proc. Natl. Acad. Sci. U.S.A. 70*, 3806.
Brown, F. F., & Campbell, I. D. (1976) *FEBS Lett. 65*, 322.
Browne, C. A., Campbell, I. D., Kiener, F. A., Phillips, D. C., Waley, S. G., & Wilson, I. A. (1976) *J. Mol. Biol. 100*, 319.
Buhler, R. H. O., & Kägi, J. H. R. (1974) *FEBS Lett. 39*, 229.
Bundi, A., & Wüthrich, K. (1977) *FEBS Lett. 77*, 11.
Bundi, A., & Wüthrich, K. (1979a) *Biopolymers 18*, 285.
Bundi, A., & Wüthrich, K. (1979b) *Biopolymers 18*, 299.
Campbell, I. D., & Dobson, C. M. (1975) *J. Chem. Soc., Chem. Commun.*, 750.
Campbell, I. D., Dobson, C. M., Williams, R. J. P., & Xavier, A. V. (1973) *J. Magn. Reson. 11*, 172.
Campbell, I. D., Dobson, C. M., & White, A. I. (1974) *J. Mol. Biol. 90*, 469.
Campbell, I. D., Dobson, C. M., Williams, R. J. P., & Wright, P. E. (1975a) *FEBS Lett. 57*, 96.
Campbell, I. D., Dobson, C. M., & Williams, R. J. P. (1975b) *Proc. R. Soc. London, Ser. B 189*, 485.
Campbell, I. D., Dobson, C. M., & Williams, R. J. P. (1975c) *Proc. R. Soc. London, Ser. A 345*, 23.
Campbell, I. D., Dobson, C. M., & Ratcliffe, R. G. (1977) *J. Magn. Reson. 27*, 455.
Dwek, R. A. (1973) *Nuclear Magnetic Resonance in Biochemistry*, Clarendon Press, Oxford.

Fiskin, A. M., Peterson, G., & Brady, F. O. (1977) *Ultramicroscopy 2*, 389.
Galdes, A., Vašák, M., Hill, H. A. O., & Kägi, J. H. R. (1978a) *FEBS Lett. 92*, 17.
Galdes, A., Hill, H. A. O., Bremner, I., & Young, B. W. (1978b) *Biochem. Biophys. Res. Commun. 85*, 217.
Glickson, J. O., Dadok, J., & Marshall, G. R. (1974) *Biochemistry 13*, 11.
Hvidt, A., & Nielsen, S. O. (1966) *Adv. Protein Chem. 21*, 287.
Kägi, J. H. R., & Vallee, B. L. (1960) *J. Biol. Chem. 235*, 3460.
Kägi, J. H. R., & Vallee, B. L. (1961) *J. Biol. Chem. 236*, 2435.
Kägi, J. H. R., Himmelhoch, S. R., Whanger, P. D., Bethune, J. L., & Vallee, B. L. (1974) *J. Biol. Chem. 249*, 3537.
Kissling, M. M., & Kägi, J. H. R. (1977) *FEBS Lett. 82*, 247.
Kojima, Y., & Kägi, J. H. R. (1978) *Trends Biochem. Sci. 3*, 90.
Kojima, Y., Berger, C., Vallee, B. L., & Kägi, J. H. R. (1976) *Prod. Natl. Acad. Sci. U.S.A. 73*, 3413.
Kopple, K. O., Ohniski, M., & Go, A. (1969) *J. Am. Chem. Soc. 91*, 4264.
Kopple, K. O., Go, A., Logan, R. H., & Savrda, J. (1972) *J. Am. Chem. Soc. 94*, 973.
Lerch, K. (1979) in *Metallothionein* (Kägi, J. H. R., & Nordberg, M., Eds.) Birkhäuser, Basel (in press).
Margoshes, M., & Vallee, B. L. (1957) *J. Am. Chem. Soc. 79*, 4813.
McDonald, C. C., & Phillips, W. D. (1969) *J. Am. Chem. Soc. 91*, 1513.
Molday, R. S., Englander, S. W., & Kallen, R. G. (1972) *Biochemistry 11*, 150.
Richards, F. M. (1963) *Annu. Rev. Biochem. 32*, 269.
Roberts, G. C. K., & Jardetzky, O. (1970) *Adv. Protein Chem. 24*, 447.
Rupp, H., Voelter, W., & Weser, U. (1974) *FEBS Lett. 40*, 176.
Sadler, P. J., Bakka, A., & Begnon, P. J. (1978) *FEBS Lett. 94*, 315.
Thiers, R. (1957) *Methods Biochem. Anal. 5*, 273.
Urry, D. W., Ohniski, M., & Walter, R. (1970) *Proc. Natl. Acad. Sci. U.S.A. 66*, 111.
Von Dreele, P. H., Brewster, A. I., Scheraga, H. A., Ferger, M. F., & Du Vigneaud, V. (1971) *Proc. Natl. Acad. Sci. U.S.A. 68*, 1028.
Von Dreele, P. H., Rae, I. O., & Scheraga, H. A. (1978) *Biochemistry 17*, 956.
Wagner, G., Wüthrich, K., & Tschesche, H. (1978) *Eur. J. Biochem. 86*, 67.
Wyssbrod, H. R., & Gibbons, W. A. (1973) *Surv. Prog. Chem. 6*, 209.

Infrared Studies on the Conformation of Synthetic Alamethicin Fragments and Model Peptides Containing α-Aminoisobutyric Acid†

Ch. Pulla Rao, R. Nagaraj, C. N. R. Rao, and P. Balaram*

ABSTRACT: Infrared studies of synthetic alamethicin fragments and model peptides containing α-aminoisobutyric acid (Aib) have been carried out in solution. Tripeptides and larger fragments exhibit a strong tendency to form β turns, stabilized by 4 → 1 10-atom hydrogen bonds. Dipeptides show less well-defined structures, though C_5 and C_7 conformations are detectable. Conformational restrictions imposed by Aib residues result in these peptides populating a limited range of states. Integrated intensities of the hydrogen-bonded N-H stretching band can be used to quantitate the number of intramolecular hydrogen bonds. Predictions made from infrared data are in excellent agreement with nuclear magnetic resonance and X-ray diffraction studies. Assignments of the urethane and tertiary amide carbonyl groups in the free state have been made in model peptides. Shifts to lower frequency on hydrogen bonding are observed for the carbonyl groups. The 1–6 segment of alamethicin is shown to adopt a 3_{10} helical structure stabilized by four intramolecular hydrogen bonds. The fragments Boc-Leu-Aib-Pro-Val-Aib-OMe (12–16) and Boc-Gly-Leu-Aib-Pro-Val-Aib-OMe (11–16) possess structures involving 4 → 1 and 5 → 1 hydrogen bonds. Supporting evidence for these structures is obtained from proton nuclear magnetic resonance studies.

The presence of α-aminoisobutyric acid (Aib)[1] in the polypeptide ionophore alamethicin (Mueller & Rudin, 1968; Martin & Williams, 1976; Pandey et al., 1977a) and the more recent demonstration of its occurrence in the closely related antibiotics suzukacillin (Jung et al., 1976), emerimicins (Pandey et al., 1977b), antiamoebins (Pandey et al., 1977c), and trichotoxin A-40 (Irmscher et al., 1978) have stimulated interest in the conformations of peptides containing Aib residues. The presence of Aib introduces considerable stereochemical constraints on the conformations of acyclic peptides. The propensity of Aib residues to initiate β turns and to generate 3_{10} helical structures has been demonstrated in solution by NMR (Nagaraj et al., 1979) and by X-ray diffraction in the solid state (Shamala et al., 1977, 1978; Prasad

† From the Solid State and Structural Chemistry Unit (Contribution No. 46) and the Molecular Biophysics Unit, Indian Institute of Science, Bangalore 560 012, India. *Received June 5, 1979.* This work has been supported by the University Grants Commission. R.N. was the recipient of a fellowship from the Department of Atomic Energy, Government of India.

* Address correspondence to this author at the Molecular Biophysics Unit.

[1] Abbreviations used: Aib, α-aminoisobutyric acid; DCC, *N,N*-dicyclohexylcarbodiimide; Z, benzyloxycarbonyl; Boc, *tert*-butyloxycarbonyl; –OMe, methyl ester; –OBz, benzyl ester.

0006-2960/80/0419-0425$01.00/0 © 1980 American Chemical Society